MODELING AND SIMULATIONS OF THIN FILM MAGNETIZED SISKO FLUID-FLOW ON AN UNSTEADY STRETCHING SURFACE

by

Ibrahim MAHARIQ[a,b,c,d], Mehreen FIZA[e], Syed Arshad ABAS[e], Hakeem ULLAH[e*], Ali AKGUL[f,g,h,i], Ghada R. ELNAGGAR[j], Ilyas KHAN[k], and Wei Sin KOH[l]

[a] College of Engineering and Architecture, Gulf University for Science and Technology, Mishref, Kuwait
[b] University College, Korea University, Seoul, South Korea
[c] Department of Medical Research, China Medical University Hospital, China Medical University, Taichung, Taiwan
[d] Applied Science Research Center, Applied Science Private University, Amman, Jordan
[e] Department of Mathematics, Abdul Wali Khan University, Mardan, Khyber Pakhtunkhwa, Pakistan
[f] Department of Electronics and Communication Engineering, Saveetha School of Engineering, SIMATS, Chennai, Tamil Nadu, India
[g] Siirt University, Art and Science Faculty, Department of Mathematics, Siirt, Turkey
[h] Applied Science Research Center, Applied Science Private University, Amman, Jordan
[i] Department of Computer Engineering, Biruni University, Topkapı, Istanbul, Turkey
[j] Department of Industrial and Systems Engineering, College of Engineering, Princess Nourah bint Abdulrahman University, Riyadh, Saudi Arabia
[k] Department of Mathematics, College of Science Al-Zulfi, Majmaah University, Al-Majmaah, Saudi Arabia
[l] INTI International University, Persiaran Perdana BBN Putra Nilai, Nilai, Negeri Sembilan, Malaysia

Original scientific paper
https://doi.org/10.2298/TSCI2504045M

The core concept revolves around the applications and mechanisms of thin film flow. Thin films are widespread, and understanding their behavior is crucial due to their extensive range of practical applications in engineering and industries. In this study 2-D thin film flow of Sisko fluid on an unsteady stretching sheet in the presence of a uniform magnetic field MHD is analyzed. The fluid moves with the stretching of the lower plate. Due to the applied magnetic field of strength Bo, the fluid is assumed to be electrically conducting. The governing equations of the flow of Sisko fluid are in the form of PDE which are converted to the ODE by the use of self-similar transformation with a non-dimensional unsteadiness factor, St. The finite element method (FEM) along with 4^{th} order Runge Kutta method (RKM-4) have been utilized to find the solution of the modeled equations. Comparison between homotopy analysis method (HAM), FEM and 4^{th} order RKM numerical procedure are shown numerically. The effect of different physical parameters on the flow profiles is discussed with a physical explanation in result and discussion section through graphs and tables. The velocity profile enhanced with the higher values of Sisko fluid parameter whereas decline with magnetic factor.

Key words: *thin film flow, unsteady stretching sheet, smart grid, MHD, FEM*

* Corresponding authors, e-mail: hakeemullah1@gmail.com; aliakgul00727@gmail.com

Introduction

The study of thin film flow has considerable attention owing to its widespread utilization across various engineering and technological domains in recent times. Thin film flow phenomena are evident in numerous fields ranging from specific instances such as air-flow in human lungs to lubrication challenges in engineering, which arguably constitutes one of the broadest areas of application. A fascinating interaction between the fields of theology, structural mechanics, and fluid mechanics is the investigation of practical applications of liquid film flow. One of its essential uses is covering wire and fiber. Researchers must prioritize the development of studies on the effects of liquid film on surface stretching in light of these potential uses. Extending the study of liquid film flow to non-Newtonian fluids builds on earlier work on viscous flow. The initial person to consider the flow of a thick fluid across a linearly expanding surface was Crane [1]. The heat transmission and viscoelastic fluid-flow on an expanding surface have been investigated by Dandapat and Gupta [2]. The initial researcher to examine the time-dependent stretching of finite liquid films was Wang [3]. Ushah and Sridharan [4] have tackled a similar issue and expanded it to a study conducted on a horizontal sheet using a liquid film fluid and heat transfer analysis. Lutera *et al.* [5] studied the exothermic reaction under the MHD effect over a porous surface.

To find a solution and talk about parameters, Liu and Andersson [6] utilized numerical methods in their study. The effect of internal heat generation in thin-film flows on a time-dependent stretching sheet was studied by Aziz *et al.* [7]. Kumar *et al.* [8] studied the MHD flow over a vertical plate, considering Soret and Dufour effect. Tawade *et al.* [9] recently investigated thin liquid flow past an unstable enlarging sheet with thermal radioactivity, in the incidence of MHD influence. There are numerous examples of thin-film flow of non-Newtonian fluids in nature. Consequently, it has grown into one of the most ubiquitous natural elements utilized mostly in engineering, technology, and industrial applications. Abas *et al.* [10] used the Casson model to studied the heat transfer properties over a stretching surface. Using the power law model, Andersson *et al.* [11] was the first to study the thin film flow of non-Newtonian fluids on an unsteady extending sheet. The investigation by Baithalu *et al.* [12] provides an in-depth analysis of magneto micro polar hybrid nanofluid-flow over an elongating surface, emphasizing the crucial roles of shear rate and couple stresses. Khan *et al.* [13] probed the liquid film flow of the nanofluid of Williamson under the influence of temperature-dependent viscosity over an unsteady stretching sheet. Andersona *et al.* [14] discussed the heat transfer phenomena in thin film flow over an unsteady stretching surface. Chen [15, 16] extend this experiment of [14] with including the power law model. The solution is obtained analytically and discussed about the effect of thin film by using power law model. While heat and viscous dissipation in MHD thin-film Oldroyd-B fluid across oscillating vertical belts is studied by Ullah *et al.* [17]. Abolbashari *et al.* [18] investigated the identical fluid using nanoparticles to generate entropy. Using Buongiorno's concept, Qasim *et al.* [19] recently investigated a fluid-thin layer on an unstable extending surface. Sisko fluid is the major subclass of non-Newtonian fluids. Asif *et al.* [20] investigated Sisko fluid in the existence of heat transmission viscous dissipation consequences and conflicting buoyancy. Khan *et al.* [21] deliberated Sisko steady fluid-flow with heat transmission in the annular pipe. Baithalu and Mishara [22] present a detailed approach that combines RSM with ANOVA to accurately determine the optimal shear rate.

Khan and Shahzad [23] examined the boundary-layer flow of a Sisko fluid above an enlarging surface. Panda *et al.* [24] used RK-4 method to study the consequences of the Darcy-

Forchheimer flow over a porous extended surface. Nadeem *et al.* [25] numerically scrutinized Maxwell fluid across an extending surface in the existence of nanoparticles with MHD. The complexity of mathematical problems in engineering and technology makes an exact solution highly difficult. Analytical and numerical approaches solve such problems. The analytical methods required small assumption of parameters, initial guess to handle the non-linear problem [26-29] with fast convergence, where the numerical methods [30-33] are equally used to handle the non-linear problems. In terms of computing efficiency, numerical techniques outweigh analytical techniques. It is possible to obtain fast and precise estimates using numerical methods. These approaches offer flexibility in solving practical issues that cannot be made simpler by making a few assumptions [34-36]. Examining the flow of Sisko-fluids, a type of liquid film, over a stretched surface while a magnetic field is present is the primary objective of this study.

In light of the cited literature, there is less study about the thin film MHD flow over an extended surface. Therefore, this paper presents a detailed study of thin film flow behavior for Sisko fluid over a time-dependent extended surface under the influence of a constant magnetic field. The fluid-flow is considered in the *x* and *y* planes and the time-dependent governing equations for Sisko fluid are reduced to ODE using similarity transformations, which incorporate the non-dimensional unsteadiness parameter. The FEM and RKM-4 recognized for its effectiveness and time-saving capabilities are used to solve the model problem. Basic equations

The leading equations of continuity and heat are stated as:

$$\operatorname{div}\hat{V} = 0 \tag{1}$$

$$\hat{\rho}\frac{\mathrm{d}\hat{V}}{\mathrm{d}t} = -\nabla p_1 + \operatorname{div}S + \boldsymbol{J}\times\boldsymbol{B},\ \frac{1}{2} \tag{2}$$

The term *S* is defined for Sisko fluid as [37, 38]:

$$S = A_1\left[c_1 + c_2\left|\sqrt{\frac{1}{2}tr\left(\boldsymbol{A}_1^2\right)}\right|^{n-1}\right] \tag{3}$$

where

$$A_1 = (\operatorname{grad}\hat{V}) + (\operatorname{grad}\hat{V})^T \tag{4}$$

where c_1, c_2 and n are the material constants which are defined differently for dissimilar fluids. The last term of eq. (2) *i.e.* $\boldsymbol{J}\times\boldsymbol{B}$ is known as Lorentz force. Here the current density is $\boldsymbol{J} = \sigma(E + V \times B)$ and magnetic field strength is denoted by B. Where σ used for electrical conductivity and $E = 0$ represent electric field. The velocity and stress profiles for 2-D flow are given as:

$$\hat{V} = \left[u_1\left(x_1, x_2\right), u_2\left(x_1, x_2\right), 0\right],\quad \hat{S} = \hat{S}\left(x_1, x_2\right) \tag{5}$$

where u_1 and u_2 along the co-ordinates axes *i.e.* x_1 and x_2 represent the velocity components.

Using eq. (5) in eqs. (1) and (2), we have:

$$\frac{\partial u_1}{\partial x_1} + \frac{\partial u_2}{\partial x_2} = 0 \tag{6}$$

$$\rho\left(u_1\frac{\partial u_1}{\partial x_1}+u_2\frac{\partial u_2}{\partial x_2}\right)=-\frac{\partial p_1}{\partial x_2}+c_1\left(\frac{\partial^2 u_2}{\partial x_1^2}+\frac{\partial^2 u_2}{\partial x_2^2}\right)+$$
$$+c_2\frac{\partial}{\partial x_2}\left[\left(\frac{\partial u_1}{\partial x_2}+\frac{\partial u_2}{\partial x_1}\right)\left|4\left(\frac{\partial u_1}{\partial x_1}\right)^2+\left(\frac{\partial u_1}{\partial x_1}+\frac{\partial u_1}{\partial x_1}\right)^2\right|^{\frac{n-1}{2}}\right]+ \tag{7}$$
$$+2c_2\frac{\partial}{\partial x_2}\left[\frac{\partial u_2}{\partial x_2}\left|4\left(\frac{\partial u_1}{\partial x_1}\right)^2+\left(\frac{\partial u_1}{\partial x_2}+\frac{\partial u_1}{\partial x_1}\right)^2\right|^{\frac{n-1}{2}}\right]$$

$$\rho\left(u_1\frac{\partial u_2}{\partial x_1}+u_2\frac{\partial u_2}{\partial x_2}\right)=-\frac{\partial p_1}{\partial x_2}+c_1\left(\frac{\partial^2 u_2}{\partial x_1^2}+\frac{\partial^2 u_2}{\partial x_2^2}\right)+$$
$$+c_2\frac{\partial}{\partial x_1}\left[\left(\frac{\partial u_1}{\partial x_2}+\frac{\partial u_2}{\partial x_1}\right)\left|4\left(\frac{\partial u_1}{\partial x_1}\right)^2+\left(\frac{\partial u_1}{\partial x_2}+\frac{\partial u_2}{\partial x_1}\right)^2\right|^{\frac{n-1}{2}}\right]+$$
$$+2c_2\frac{\partial}{\partial x_2}\left[\frac{\partial u_2}{\partial x_2}\left|4\left(\frac{\partial u_1}{\partial x_1}\right)^2+\left(\frac{\partial u_1}{\partial x_2}+\frac{\partial u_2}{\partial x_1}\right)^2\right|^{\frac{n-1}{2}}\right] \tag{8}$$

In eqs. (7) and (8) if $a = 0$ and $b = 0$ then the fluid change to power law and Newtonian fluids respectively. Introduce the dimensionless variable as [38]:

$$u_1^{*}=\frac{u_1}{U},\quad u_2^{*}=\frac{u_2}{U},\quad x_1^{*}=\frac{x_1}{L},\quad x_2^{*}=\frac{x_2}{L}\quad\text{and}\quad p_1^{*}=\frac{p_1}{\rho U^2} \tag{9}$$

Using eqs (9), eqs. (6) and (7) are written as:

$$u_1^{*}\frac{\partial u_1^{*}}{\partial x_1^{*}}+u_2^{*}\frac{\partial u_2^{*}}{\partial x_2^{*}}=-\frac{\partial p_1^{*}}{\partial x_1^{*}}+\varepsilon_1\left(\frac{\partial^2 u_1^{*}}{\partial x_1^{*2}}+\frac{\partial^2 u_1^{*}}{\partial x_2^{*2}}\right)+$$
$$2\varepsilon_2\frac{\partial}{\partial x_1^{*}}\left[\frac{\partial u_1^{*}}{\partial x_1^{*}}\left|4\left(\frac{\partial u_1^{*}}{\partial x_1^{*}}\right)^2+\left(\frac{\partial u_1^{*}}{\partial x_2^{*}}+\frac{\partial u_2^{*}}{\partial x_1^{*}}\right)^2\right|^{\frac{n-1}{2}}\right]+$$
$$\varepsilon_2\frac{\partial}{\partial x_2^{*}}\left[\left(\frac{\partial u_1^{*}}{\partial x_2^{*}}+\frac{\partial u_2^{*}}{\partial x_1^{*}}\right)\left|4\left(\frac{\partial u_1^{*}}{\partial x_1^{*}}\right)^2+\left(\frac{\partial u_1^{*}}{\partial x_2^{*}}+\frac{\partial u_2^{*}}{\partial x_1^{*}}\right)^2\right|^{\frac{n-1}{2}}\right] \tag{10}$$

$$u_1^* \frac{\partial u_2^*}{\partial x_1^*} + u_2^* \frac{\partial u_2^*}{\partial x_2^*} = -\frac{\partial p_1^*}{\partial x_2^*} + \varepsilon_1 \left(\frac{\partial^2 u_2^*}{\partial x_1^{*2}} + \frac{\partial^2 u_2^*}{\partial x_2^{*2}} \right) +$$

$$+\varepsilon_2 \frac{\partial}{\partial x_1^*} \left[\left(\frac{\partial u_1^*}{\partial x_2^*} + \frac{\partial u_2^*}{\partial x_1^*} \right) \left| 4 \left(\frac{\partial u_1^*}{\partial x_1^*} \right)^2 + \left(\frac{\partial u_1^*}{\partial x_2^*} + \frac{\partial u_2^*}{\partial x_1^*} \right)^2 \right|^{\frac{n-1}{2}} \right] +$$

$$+2\varepsilon_2 \frac{\partial}{\partial x_2^*} \left[\frac{\partial u_2^*}{\partial x_2^*} \left| 4 \left(\frac{\partial u_1^*}{\partial x_1^*} \right)^2 + \left(\frac{\partial u_1^*}{\partial x_2^*} + \frac{\partial u_2^*}{\partial x_1^*} \right)^2 \right|^{\frac{n-1}{2}} \right] \tag{11}$$

The dimensionless factors ε_1 and ε_1 are defined as:

$$\varepsilon_1 = \frac{a}{\rho LU} \quad \text{and} \quad \varepsilon_2 = \frac{b}{\rho LU} \left(\frac{U}{L} \right)^{n-1} \tag{12}$$

The following equations are transformed into their dimensional form using the boundary-layer approximations:

$$\rho \left(u_1 \frac{\partial u_1}{\partial x_1} + u_2 \frac{\partial u_1}{\partial x_2} \right) = -\frac{\partial p_1}{\partial x_1} + c_1 \frac{\partial^2 u_1}{\partial x_2^2} + c_2 \frac{\partial}{\partial x_2} \left(\left| \frac{\partial u_1}{\partial x_2} \right|^{n-1} \frac{\partial u_1}{\partial x_2} \right) \tag{13}$$

$$0 = -\frac{\partial p_1}{\partial x_2} \tag{14}$$

Mathematical description of problem

The Sisko fluid electric conductivity and time-dependent liquid film flow are taken into account while the surface is being spread.

The co-ordinate axes are designated in such a way that the x_1-axis is the direction of the flow while the x_2-axis is normal to the sheet correspondingly as shown schematically in fig. 1.

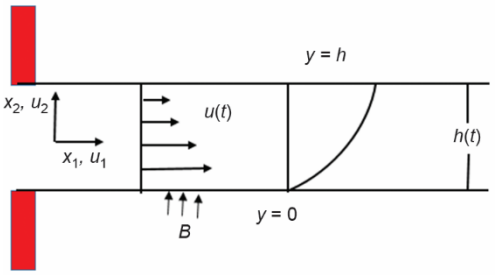

Figure 1. The physical configuration of the modelled problem

The surface of the fluid is stretched where two forces having oppositive directions and the same magnitude are acting along the x_1-axis and maintain the origin stagnant. The sheet is stretched I in x_1-axis with velocity:

$$U_w(x_1, t) = cx_1 (1 - \chi t)^{-1} \tag{15}$$

where c and χ are constants greater than zero. The x_2-axis is perpendicular to it. The time-dependent term, *St*, is the local Reynold number, which relies on the surface velocity $U_w(x_1, t)$ initially the slit is at rest with the origin and after some time it is stretched along x_1-axis by an

external force at the rate of $c(1 - \chi t)^{-1}$. A magnetic field of variable type is perpendicular to the sheet and defined as:

$$B(t) = B_0 \left(1 - \chi t\right)^{-1/2} \tag{16}$$

The leading flow equations along with boundary conditions are [38-40]:

$$\frac{\partial u_1}{\partial x_1} + \frac{\partial u_2}{\partial x_2} = 0 \tag{17}$$

$$\frac{\partial u_1}{\partial t} + u_1 \frac{\partial u_1}{\partial x_1} + u_2 \frac{\partial u_1}{\partial x_2} = \frac{c_1}{\rho} \frac{\partial^2 u_1}{\partial {x_2}^2} - \frac{c_2}{\rho} \frac{\partial}{\partial x_2} \left(-\frac{\partial u_1}{\partial x_2} \right)^n - \sigma B^2(t) u_1 \tag{18}$$

The associated boundary conditions are:

$$\begin{aligned} &u_1 = U_w, \quad u_2 = 0, \quad \text{at } x_2 = 0 \\ &\frac{\partial u_1}{\partial x_1} = 0, \quad u_2 = \frac{\mathrm{d}h}{\mathrm{d}t}, \quad \text{at } x_2 = h \end{aligned} \tag{19}$$

were u_1 and u_2 denote the components of velocity, the density is ρ and $B(t)$ strength of the magnetic field.

Similarity variables

Introducing the dimensionless and similarity variables are f and η, respectively, for subsequent transformation as [40]:

$$f\left(\eta\right) = \psi(x_1, x_2, t) \left(\frac{1 - \chi t}{\nu c} \right)^{0.5}, \quad \eta = \left[\frac{c}{\nu(1 - \chi t)} \right]^{0.5} x_2, \quad h(t) = \left[\frac{\nu\left(1 - \chi t\right)}{c} \right]^{0.5} \tag{20}$$

where $\psi(x_1, x_2, t)$ specify the stream function, $h(t)$ specify the thin film thickness and $\nu (= \mu/\rho)$ the kinematics viscosity.

$$u_1 = \frac{\partial \psi}{\partial x_2} = \left(\frac{c x_1}{1 - \chi t} \right) f'\left(\eta\right), \quad x_2 = -\frac{\partial \psi}{\partial x_1} = -\left(\frac{\nu c}{1 - \chi t} \right)^{1/2} f\left(\eta\right) \tag{21}$$

Applying the similarity variables of eq. (7) into eqs. (1)-(6) the transformed non-linear differential equation as:

$$\varepsilon f''' + \left(f - \frac{St\eta}{2} \right) f'' - \left(St + M + f' \right) f' + n\xi \left(-f'' \right)^{n-1} f''' = 0 \tag{22}$$

The transformed boundary constraints are:

$$f(0) = f''(\beta) = 0, \quad f'(0) = 1, \quad f(\beta) = \frac{S\beta}{2} \tag{23}$$

The film thickness:

$$\beta = \left[\frac{b}{\nu(1-\chi t)}\right]^{1/2} h(t)$$

which gives:

$$\frac{\mathrm{d}h}{\mathrm{d}t} = -\frac{\alpha\delta}{2}\left[\frac{b(1-\alpha t)}{\nu}\right]^{-0.5} \tag{24}$$

The physical non-dimensionalless constraints are, the unsteadiness factor is St (= β/c), the Sisko fluid factor is ε [= $a/(\rho\nu)$], the stretching factor is:

$$\xi\left(=\frac{b}{\rho\nu}\left\{\left[\frac{cx}{(1-\beta t)\sqrt{\nu}}\right]^{3/2}\right\}^{n-1}\right)$$

and the magnetic factor is:

$$M\left(=\frac{\sigma_f B_0^2}{b\rho_f}\right)$$

Solution procedure

The FEM is a potent approach for tackling non-linear differential equations, applicable across various engineering domains including fluid mechanics, biomathematics, physics, and channel processes.

Consider a non-linear ODE [41]:

$$\frac{\mathrm{d}^3 f}{\mathrm{d}\eta^3} + g(\chi, f, f', f'') = s(\chi,\eta) \tag{25}$$

with boundary conditions:

$$f(a) = f_a, \quad f'(a) = f_a', \quad f(b) = f_b \tag{26}$$

where

$$g(\chi, f, f', f'') = \sum_{m=0}^{M}\sum_{n=0}^{N} d_{m,n}(\chi) f^m \left(\frac{\mathrm{d}f}{\mathrm{d}\eta}\right)^n \tag{27}$$

is non-linear function. Using the Galerkin FEM for eq. (25), we have:

$$\int_{\delta} w(\eta)\left[\frac{\mathrm{d}^3 f}{\mathrm{d}\eta^3} + g(\chi, f, f', f'') - s(\chi,\eta)\right]\mathrm{d}\eta = 0 \tag{28}$$

where $w(\eta)$ is the weight function and δ is the domain of the problem. From eq. (28), we have:

$$\sum_{e=1}^{M}\int_{\delta} w(\eta)\, g(\chi)\,\mathrm{d}\eta - \sum_{e=1}^{M}\int_{\delta} w(\eta)\frac{\mathrm{d}f}{\mathrm{d}\eta}\xi_\eta \mathrm{d}\delta \tag{29}$$

where ξ_n is the compoenent of unit outward normal of the boundary.

The function f at any point is approximated by:

$$f(\eta,\chi)=\sum_{l=1}^{M_h} f_l(\chi)s_l(\eta) \tag{30}$$

where M_h represents the number of nodes, $f_l(\chi)$ are the nodal unkown value of f and $s_l(\eta)$ are the shape function defined as:

$$s_l(\eta)=\begin{cases}1 & m=n\\ 0 & m\neq n\end{cases} \tag{31}$$

$$w(\eta)=s_l(\eta) \tag{32}$$

using eq. (29) and eq. (32), we have:

$$\sum_{e=1}^{M}\int_{\delta} s_l(\eta)g(\chi)\mathrm{d}\eta-\sum_{e=1}^{M}\int_{\delta} s_l(\eta)\frac{\mathrm{d}f}{\mathrm{d}\eta}\xi_\eta\mathrm{d}\delta \tag{33}$$

The non-linear term can be calculated as:

$$g(\chi,f,f',f'')=d_{0,0}(\chi)+\sum_{m=0}^{M} d_{m,0}(\chi)\bar{f}^{m-1}+\sum_{n=0}^{N} d_{0,m}(\chi)\left(\frac{\mathrm{d}\bar{f}}{\mathrm{d}\eta}\right)^{n-1}\frac{\mathrm{d}\bar{f}}{\mathrm{d}\eta}+$$
$$+\sum_{m=1}^{M}\sum_{n=1}^{N} d_{n,m}(\chi)\bar{f}^{m}\left(\frac{\mathrm{d}\bar{f}}{\mathrm{d}\eta}\right)^{n-1}\frac{\mathrm{d}\bar{f}}{\mathrm{d}\eta} \tag{34}$$

where

$$\bar{f}=\sum_{l=1}^{M_h}\bar{f}_l(\chi)s_l(\eta) \tag{35}$$

is the initial guess. Equation (33) results in a system of non-linear algebraic equations. By solving these system of equations, we obtain the unkown nodal values as a function of χ. Once the nodal values are obtain then the solution is obtain for the entire domain.

Results and discussion

This section aims to examine how different physical parameters influence the velocity $f(\eta)$ distributions. The FEM solution is compared with numerical results 4th order RK method for accuracy. Figure 2 spectacles the effect of unsteady constraint *St* in the presence of different values of the of power index n (= 0, 1, 2) on $f(\eta)$. When the snowballing *St* the $f(\eta)$ profile climbs. A higher power index value results in a more pronounced acceleration of the velocity distribution, thus it is evident that changing the power index has the same effect as changing the unstable parameter. It is observed that the solution is dependent on the unsteadiness parameter with a solution range. As *St* enhanced the motion of the nanofluid is escalates. Similarly altering the power index has a comparable effect on the unsteadiness parameter where an increase in the power index leads to a rise in the velocity distribution. Figure 3 demonstrates the impact of film thickness β for changing n (= 0, 1, 2). In coating processes, β is a critical factor, as it significantly impacts performance. Physically, β is directly influenced by the velocity of the fluid. It is noted that the $f(\eta)$ profile drops with ascending values of β. Actually fluid film offers resistance to the flow with the higher values of β and goes to slow down $f(\eta)$. The reason is that the film thickness and viscosity are directly related to each other.

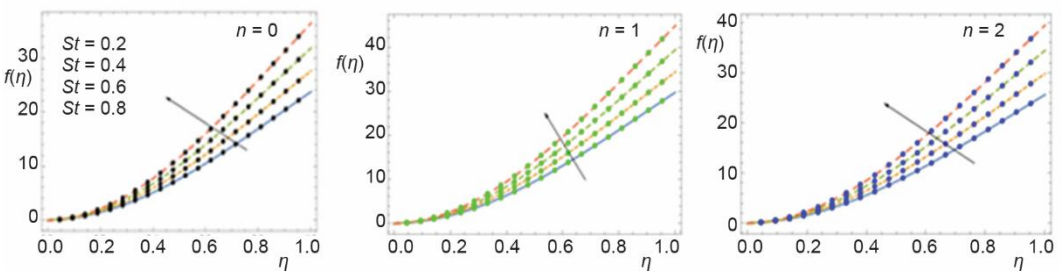

Figure 2. Effect of *St* on *f*(*η*) for *n* = 0, 1, 2, 3, when *β* = 0.8, *ξ* = 0.3, *M* = 1.0, and *ε* = 0.2

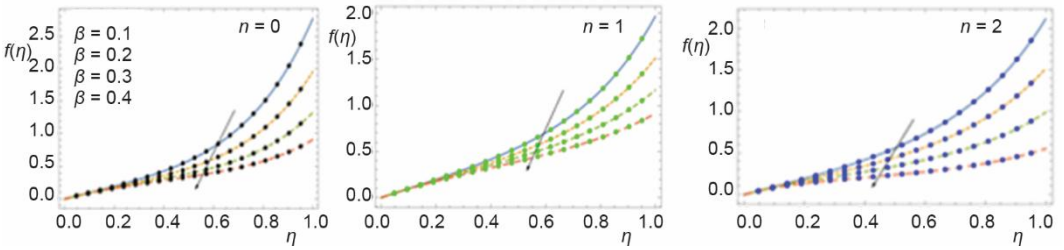

Figure 3. Influence of *β* on *f*(*η*) for *n* = 0, 1, 2, 3, when *St* = 0.4, *ε* = 0.2, *ξ* = 0.3, and *M* = 1.0

Figure 4 describe the impact of the magnetic factor, *M*, on *f*(*η*) for various numbers of *n* (= 0, 1, 2). When *M* escalates the *f*(*η*) surpresses on the sheet surface. The application of a magnetic field to a fluid causes it to exhibit these phenomena because it generates a resistive force known as the Lorentz force. This force act perpendicular to the fluid motion. Hence creates an obstacle in flow direction. Thus this force causes the fluid's velocity to slow down. Figure 5 demonstrates that the impact of the stretching factor ε for changing values of *n*(1, 2, 3) on *f*(*η*) profile. The *f*(*η*) profile increase for growing value of *ε* when *n*(= 1) when values changes from 1 to 3, the effect of extending parameter *ε* also changed and for *n* = 3 the stretching factor has oppositive impact on *f*(*η*) that is *f*(*η*) diminishes. For *n* = 0 then *ε* will become zero. The effect of *ε* for different values of *n* on *f*(*η*) is revealed in fig. 6. The higher values of *ε* enhance fluid motion, but as the power index increases *n* = 3 this effect undergoes a change resulting in a reduction in the *f*(*η*) field. Moreover, the velocity profile escalates as the value of *ε* climbs, since the lower plate directly influences the fluid velocity. Physically when $\varepsilon > 0$, the surface acceleration escalates, when $\varepsilon < 0$ the surface decelerates when $\varepsilon = 0$ the surface exhibits random motion.

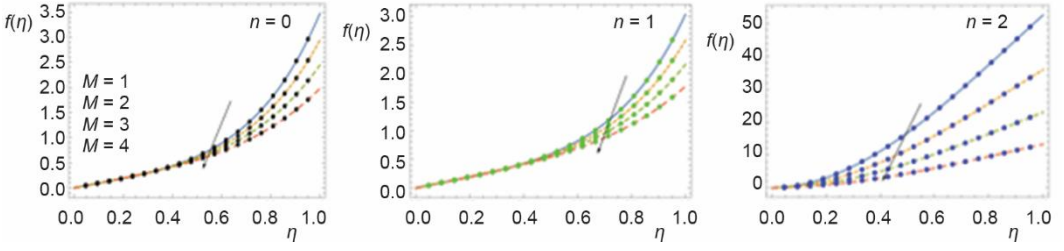

Figure 4. Influence of *M* on *f*(*η*) for *n* = 0, 1, 2, 3, when *St* = 0.4, *ε* = 0.2, and *ξ* = 0.3

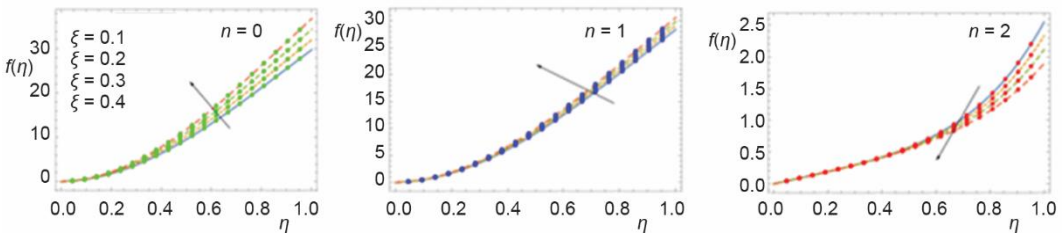

Figure 5. Influence of ξ on $f(\eta)$, when $\beta = 0.8$, $\varepsilon = 0.2$, $St = 0.4$, and $M = 1.0$

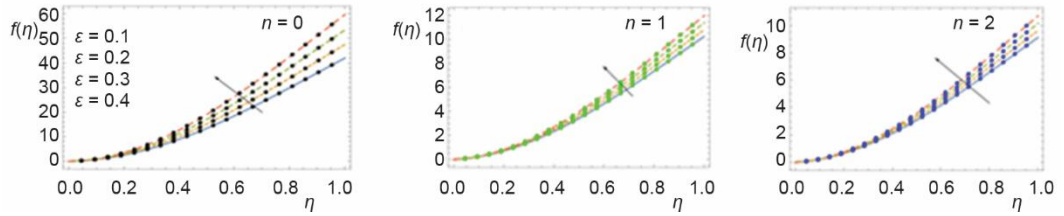

Figure 6. Influence of ε on $f(\eta)$, when $\beta = 0.4$, $St = 0.4$, $M = 1.0$, and $\xi = 0.2$

Validation of results

The modeled equations, along boundary conditions, are solved numerically and analytically. A comparison among HAM, RKM-4, and FEM solutions are presented both graphically and numerically for velocity. Figure 7 shows an excellent agreement between RKM-4 and the numerical method. Additionally, tabs. 1-3 confirm the accuracy of the results obtained

Table 1. The association between HAM, FEM, and RK method for $f(\eta)$ in case of $n = 0$, when $\beta = \varepsilon = 1$, $St = M = 0.1$, and $\xi = 0.8$

η	RK method order 4	FEM solution	HAM [30]	Absolute error
0	0.00000	0.0000000	0.00000	0.0000000
0.1	0.096682	0.096682	0.096797	$-1.5\cdot10^{-04}$
0.2	0.187429	0.187429	0.187874	$-4.46\cdot10^{-04}$
0.3	0.273169	0.273169	0.274142	$-9.73\cdot10^{-04}$
0.4	0.354701	0.354701	0.356381	$-1.68\cdot10^{-03}$
0.5	0.432726	0.432726	0.4352750	$-2.549\cdot10^{-03}$
0.6	0.507882	0.507882	0.511437	$-3.555\cdot10^{-03}$
0.7	0.589755	0.580755	0.585433	$-4.678\cdot10^{-03}$
0.8	0.651911	0.651911	0.657798	$5.887\cdot10^{-03}$
0.9	0.721905	0.721905	0.729058	$-7.153\cdot10^{-03}$
1	0.791305	0.791305	0.799754	$-8.449\cdot10^{-03}$

Table 2. The association between HAM, FEM, and RK numerical techniques for $f(\eta)$ in case of $n = 1$, when $\beta = \varepsilon = 1$, $St = M = 0.1$, and $\xi = 0.8$

η	RK Method	FEM solution	HAM [30]	Absolute error
0	0.00000	0.00000	0.0000	0.0000000
0.1	0.096941	0.096941	0.096797	$-2.15462\cdot10^{-04}$
0.2	0.192135	0.192135	0.187875	$-1.52485\cdot10^{-04}$
0.3	0.273169	0.273169	0.274142	$-1.25478\cdot10^{-04}$
0.4	0.354701	0.354701	0.356381	$-3.214568\cdot10^{-04}$
0.5	0.432726	0.432726	0.435275	$-1.95483\cdot10^{-04}$
0.6	0.507882	0.507882	0.511437	$-5.21002\cdot10^{-04}$
0.7	0.580755	0.580755	0.585433	$-1.8523\cdot10^{-03}$
0.8	0.651911	0.651911	0.657798	$1.0215\cdot10^{-03}$
0.9	0.721905	0.721905	0.729058	$-1.8526\cdot10^{-03}$
1	0.791305	0.791305	0.799754	$-1.98752\cdot10^{-03}$

Table 3. Comparison of solution of $f(\eta)$ in case of $n = 2$, when $\beta = \varepsilon = 1$, $St = M = 0.1$, and $\xi = 0.8$

η	RK Method	FEM solution	HAM [30]	Absolute error
0	1.00000	1.00000	1.00000	0.000000
0.1	1.04865	1.04865	1.05256	$3.9\cdot10^{-03}$
0.2	1.09068	1.09068	1.09617	$5.5\cdot10^{-03}$
0.3	1.12653	1.12653	1.13199	$5.5\cdot10^{-03}$
0.4	1.15656	1.15656	1.161	$4.4\cdot10^{-03}$
0.5	1.18115	1.18115	1.18401	$2.9\cdot10^{-03}$
0.6	1.20063	1.20063	1.20172	$1.1\cdot10^{-03}$
0.7	1.21532	1.21532	1.21472	$6.0\cdot10^{-04}$
0.8	1.2255	1.2255	1.2235	$2.0\cdot10^{-03}$
0.9	1.23144	1.23144	1.22851	$2.9\cdot10^{-03}$
1.0	1.23337	1.23337	1.2301	$3.8\cdot10^{-03}$

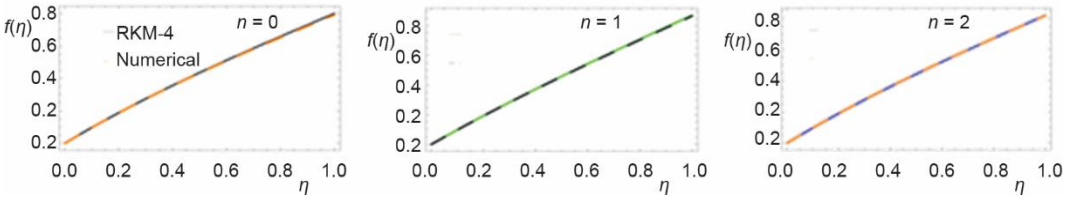

Figure 7. Comparison graphs when $\xi = 0.8$, $\beta = 1$, $\varepsilon = 1$, $h = -0.6$, $St = 0.1$, $M = 0.1$

from FEM with RK Method of order 4 along with HAM results. From the comparison it is clear that the FEM results are very close to the RK method of order which confirms the accuracy and validity of the method. The effect of M, ξ, β, and St on C_f are given in tab. 4. It is observed that growing values of M, ξ, and β lessening C_f while mounting St intensify the skin friction as given in tab. 4. The higher magnetic field generates the Lorentz force which is responsible for the declination in the velocity of the fluid. As a result, the skin friction of the fluid improved.

Table 4. The C_f for dissimilar values of M, k, β, and S

M	ξ	β	St	$f''(0)$ $n = 0$	$f''(0)$ $n = 1$	$f''(0)$ $n = 2$	$f''(0)$ $n = 3$
0.1	0.5	1.0	1.5	2.6702	2.6702	3.1102	3.3302
0.5				1.9476	2.6472	2.9988	2.9488
1.0				1.7420	2.4421	2.6728	2.6428
1.5	0.1			2.1299	2.3291	3.4399	4.3399
	0.5			2.3215	2.3223	3.4115	4.3215
	1.0			2.2087	2.2001	3.2087	4.2687
	1.5	1.0		2.6921	2.6957	4.6992	5.6422
		1.0		2.1453	2.1453	4.5556	5.4456
		1.0		2.3986	2.1986	3.8871	4.8911
		1.0	0.1	2.1273	2.1272	3.0173	4.1273
			0.5	2.3592	2.3392	3.3472	4.3572
			1.0	2.5048	2.5048	4.5765	5.1048
			1.5	2.9120	3.0020	5.1982	5.9122

Conclusions

This section contains the main findings of different physical parameters on the 2-D thin film flow of Sisko fluid on an unsteady stretching sheet in the presence of a uniform magnetic field MHD. The fluid is assumed to be electrically conducting. The governing equa-

tions of the flow of Sisko fluid are in the form of PDE which are converted to the ODE by the use of self-similar transformation with a non-dimensional unsteadiness factor. The modeled equations have been solved through FEM and numerical methods. The impact of the embedded parameter is visually and analytically examined. The key remarks are:

- The velocity field declined with higher magnetic parameter, while an increasing behaviour is noted for the Sisko and parameters.
- The validation of the solution obtained via FEM has been confirmed using numerical methods.
- A higher power index value results in a more pronounced acceleration of the velocity distribution, thus it's evident that changing the power index has the same effect as changing the unstable parameter.
- The higher values of enhance fluid motion, but as the power index increases this effect reverse.
- The higher values of unsteady constraint in the presence of different values of the power index escalate velocity profile.
- Higher values of *n* provide a greater range in velocity between the centerline and the boundary, whereas lower values of n result in a more uniform velocity profile.
- Sisko fluid flow is dampened by the magnetic field, which lowers velocities and modifies velocity profiles. As the intensity of the magnetic field rises, these effects become more noticeable.

Acknowledgment

The authors extend their appreciation to the support of funding received from Princess Nourah bint Abdulrahman University Researchers Supporting Project number (PNURSP2025R914), Princess Nourah bint Abdulrahman University, Riyadh, Saudi Arabia.

References

[1] Crane, L. J., Flow Past a Stretching Plate, *Angrew. Math. Phys., 21* (1970), July, pp. 645-647
[2] Dandapat, B. S., Gupta, A. S., Flow and Heat Transfer in a Viscoelastic Fluid over a Stretching Sheet, *Int. J. Nonlinear Mech. 24* (1989), 3, pp. 215-219
[3] Wang, C. Y., Liquid Film on an Unsteady Stretching Surface, *Q Appl Math., 48* (1990), 4, pp. 601-610
[4] Usha, R., Sridharan, R., On the Motion of a Liquid Film on an Unsteady Stretching Surface, *ASME Fluids Eng., 150* (1993), pp. 43-48
[5] Lutera, J. N., *et al*., Analyzing the Exothermic Reactions of Cu Nanoparticles with the Dufour Effect and the Influence of the Heat Generation and Permeability Past a Porous Moving Surface, *Results in Chemistry, 10* (2024), 101730
[6] Liu, I. C., Andersson, I. H., Heat Transfer in a Liquid Film on an Unsteady Stretching Sheet, *International Journal of Thermal Sciences, 47* (2008), 6, pp. 766-772
[7] Aziz, R. C., *et al.*, Thin Film Flow and Heat Transfer on an Unsteady Stretching Sheet with Internal Heating, *Meccanica, 46* (2011), June, pp. 349-357
[8] Kumar, V. V., *et al*., Role of Soret, Dufour Influence on Unsteady MHD Oscillatory Casson Fluid Flow an Inclined Vertical Porous Plate in the Existence of Chemical Reaction, *Journal of Advanced Research in Fluid Mechanics and Thermal Sciences, 110* (2023), 2, pp. 157-175
[9] Tawade, L., *et al*., Thin Film Flow and Heat Transfer over an Unsteady Stretching Sheet with Thermal Radiation, Internal Heating in Presence of External Magnetic Field, *Int. J. Adv. Appl. Math. And Mech., 3* (2016), Mar., pp. 29-40
[10] Abas, S. A., *et al*., A Passive Control of Magnetohydrodynamic Flow of a Blood-Based Casson Hybrid Nanofluid over a Convectively Heated Bi-Directional Stretching Surface, *ZAMM-Journal of Applied Mathematics and Mechanics/Zeitschrift für Angewandte Mathematik und Mechanik, 104* (2024), 1, 202200576

[11] Andersson, H. I., *et al.*, Flow of a Power-Law Fluid Film on an Unsteady Stretching Surface, *J. Non-Newtonian Fluid Mech., 62* (1996), 1, pp. 1-8
[12] Baithalu, R., *et al.*, Optimizing Shear and Couple Stress Analysis for the Magneto-Micropolar Dissipative Nanofluid Flow toward an Elongating Surface: a Comprehensive RSM-ANOVA Investigation, *Journal of Thermal Analysis and Calorimetry, 149* (2024), 4, pp. 1697-1713
[13] Khan, W., *et al.*, Thin Film Williamson Nanofluid Flow with Varying Viscosity and Thermal Conductivity on a Time-Dependent Stretching Sheet, *Appl. Sci., 6* (2016), 11, 334
[14] Anderssona, H. I., *et al.*, Heat Transfer in a Liquid Film on an Unsteady Stretching, *International Journal of Heat and Mass Transfer 43* (2000), 1, pp. 69-74
[15] Chen, C. H., Heat Transfer in a Power-Law Liquid Film over a Unsteady Stretching Sheet, *Heat and Mass Transfer, 39* (2003), Oct., pp. 791-796
[16] Chen, C. H., Effect of Viscous Dissipation on Heat Transfer in a non-Newtonian Liquid Film over an Unsteady Stretching Sheet, *J. Non-Newtonian Fluid Mech., 135* (2006), 2-3, pp. 128-135
[17] Ullah, H., *et al.*, MHD thin Film Oldroyd-b Fluid with Heat and Viscous Dissipation over Oscillating Vertical Belts, *Heat Transfer Research, 50* (2019), 8, pp. 1-11
[18] Abolbashari, M. H., *et al.*, Analytical Modeling of Entropy Generation for Casson Nanofluid-flow Induced by a Stretching Surface, *Advanced Powder Technology, 26* (2015), 2, pp. 542-552
[19] Qasim, M., *et al.*, Heat and Mass Transfer in Nanofluid Thin Film over an Unsteady Stretching Sheet Using Buongiorno's Model, *Eur. Phys. J. Plus. 131* (2016), 16
[20] Asif, M., *et al.*, Mixed Convection Heat Transfer in Sisko Fluid with Viscous Dissipation, Effects of Assisting and Opposing Buoyancy, *Chem. Engin. Rsearch and Design, 97* (2015), May, pp. 120-127
[21] Khan, M., *et al.*, Steady Flow and Heat Transfer of a Sisko Fluid in Annular Pipe, *International Journal of Heat and Mass Transfer, 53* (2010), 7-8, pp. 1290-1297
[22] Baithalu, R., Mishra, S. R., On Optimizing Shear Rate Analysis for the Water-Based CNT Micropolar Nanofluids via an Elongating Surface: Response Surface Methodology Combined with ANOVA test, *Journal of Thermal Analysis and Calorimetry, 148* (2023), 24, pp.14275-14294
[23] Khan, M., Shahzad, A., On Boundary Layer Flow of a Sisko Fluid over a Stretching Sheet, *Quaestiones Mathematicae, 36* (2013), 1, pp. 137-151
[24] Panda, S., *et al.*, Inertial Drag Combined with Nonuniform Heat Generation/Absorption Effects on the Hydromagnetic Flow of Polar Nanofluid over an Elongating Permeable Surface due to the Impose of Chemical Reaction, *ZAMM, Journal of Applied Mathematics and Mechanics/Zeitschrift für Angewandte Mathematik und Mechanik, 104* (2024), 9, e202301058
[25] Nadeem, S., *et al.*, Numerical Study of MHD Boundary Layer Flow of a Maxwell Fluid past a Stretching Sheet in the Presence of Nanoparticles, *Journal of the Taiwan Institute of Chemical Engineers, 45* (2014), 1, pp. 121-126
[26] Mumtaz, M., *et al.*, Chemically Reactive MHD Convective Flow and Heat Transfer Performance of Ternary Hybrid Nanofluid past a Curved Stretching Sheet, *Journal of Molecular Liquids, 390* (2023) Part B, 123179
[27] Ullah, H., *et al.*, Solution of Boundary Layer Problems with Heat Transfer by Optimal Homotopy Asymptotic Method, *Abst. Appl. Anal., 2* (2013), 324869
[28] Ullah, H., *et al.*, Application of Optimal Homotopy Asymptotic Method to Burger Equations, *J. Appl. Math., 2* (2013), 387478
[29] Ullah, H., *et al.*, Optimal Homotopy Asymptotic Method to Nonlinear Damped Generalized Regularized Long Wave Equation, *Math. Prob. Engi., 2* (2013), 503137
[30] Liao, S. J., On Homotopy Analysis Method for Nonlinear Problems, *Appl. Math. Comput., 147* (2004), 2, pp. 499-513
[31] Dhairiyasamy, R., *et al.*, Impact of Silver Nanofluid Modifications on Heat Pipe Thermal Performance, *J Therm. Anal. Calorim., 150* (2025), Jan., pp. 2079-2098
[32] Hai, T., *et al.*, Optimizing Ternary Hybrid Nanofluids Using Neural Networks, Gene Expression Programming, and Multi-Objective Particle Swarm Optimization: a Computational Intelligence Strategy, *Sci. Rep., 15* (2025), 1986
[33] Xiang, J., *et al.*, Development of Novel Thermal Diode Based on Improved Check Valve and Modified Wick Structure, *International Journal of Thermal Sciences, 200* (2024), 108977
[34] Hou, Y., *et al.*, Unsteady Conjugate Heat Transfer Simulation of Wall Heat Loads for Rotating Detonation Combustor, *International Journal of Heat and Mass Transfer, 221* (2024), 125081

[35] Chen, X., *et al.*, Manipulation of the Flow Induced by Afterbody Vortices Using Sweeping Jets, *Physics of Fluids, 36* (2024), 3, 035147
[36] Mumtaz, M., *et al.*, A Numerical Approach to Radiative Ternary Nanofluid Flow on Curved Geometry with Cross-Diffusion and Second Order Velocity Slip Constraints, *International Journal of Heat and Fluid Flow 105* (2024), 109255
[37] Darji, R. M., Timol, M. G., Similarity Analysis for Unsteady Natural Convective Boundary Layer flow of Sisko Fluid, *Int. J. Adv. Appl. Math. Mech., 1* (2014), 3, pp. 22-36
[38] Patel, M., *et al.*, Laminar Boundary Flow of Sisko Fluid, *Int. J. Appl. And Appl. Math., 10* (2015), 2, pp. 909-918
[39] Olanrewaju, O., *et al.*, Unsteady Free Convective Flow of Sisko Fluid with Radiative Heat Transfer past a Flat Plate Moving through a Binary Mixture, *Thermal Energy and Power Engineering, 10* (2013), 2, pp. 109-117
[40] Jawad, M., *et al.*, Nanofluid Thin Film Flow of Sisko Fluid and Variable Heat Transfer over an Unsteady Stretching Surface with External Magnetic Field, *Journal of Algorithms & Computational Technology, 13* (2019), 1748301819832456
[41] Ibrahim, E., *et al.*, Finite Element Method for Solving Nonlinear Random Ordinary Differential Equations, *Matrix Science Mathematic, 3* (2019), 2, pp. 17-21

Paper submitted: November 11, 2024
Paper revised: February 14, 2025
Paper accepted: April 27, 2025